Dynamics of Hairy-Rod Polymers: Semidilute Regime

G. Petekidis,† D. Vlassopoulos,* and G. Fytas

Foundation for Research and Technology−Hellas, Institute of Electronic Structure and Laser, P.O. Box 1527, 71110, Heraklion, Crete, Greece

G. Fleischer

Universität Leipzig, Fakultät für Physik und Geowissenschaften, D-04103 Leipzig, Germany

Received July 28, 1997; Revised Manuscript Received October 1, 1997

ABSTRACT: Photon correlation spectroscopy was employed in both the polarized (VV) and depolarized (VH) geometries in order to investigate the dynamics of concentration and orientation fluctuations of model hairy-rod poly(*p*-phenylenes) in semidilute solution. These materials possess a large inherent optical anisotropy, which allowed the unambiguous detection of orientation relaxation. By probing the dynamics in two solvents of different qualities, chloroform, a good solvent, and toluene, it was possible to distinguish nearly molecular from aggregate processes. Two modes were detected in the VV correlation function: the fast cooperative diffusion, D_c, which increased nearly linearly with concentration ($D_c/D_0 - 1 \sim c^{0.9}$), and a slow mode, D_{slow}, which slowed with concentration ($D_{slow} \sim c^{-1}$). The latter process was assigned to the self-diffusion of small aggregates, as confirmed by independent pulsed field gradient NMR measurements. Broad VH correlation functions were obtained at high concentrations and revealed the presence of a dominant mode exhibiting a decay rate, Γ_{VH}, which decreased with increasing q and concentration ($\Gamma_{VH} \sim c^{-0.25}$). This mode was assigned to orientational correlations in space, due to some local ordering of parts of the molecules. These findings cannot be accounted for by the existing theories.

I. Introduction[2]

The basic features of rigid-rod polymers, which make them technologically important and scientifically challenging, in particular with respect to biological applications, are associated with their highly anisotropic shape, the formation of mesophases, their anisotropic diffusion, and the translation−rotation coupling. These pertinent characteristics have been predicted theoretically and investigated experimentally.[1−4] However, the dynamic behavior of these stiff-chain molecules, affected by the above features, still represents an unresolved issue, in particular as the isotropic-to-nematic transition is approached. Typically, the collective dynamics of polymers in solution is probed experimentally by photon correlation spectroscopy (PCS), which in the polarized geometry (VV) reveals the isotropic concentration fluctuations and in the depolarized geometry (VH) the orientational fluctuations. In contrast to flexible macromolecules, rodlike polymers have received much less attention, despite the fact that their anisotropic shape can offer, in principle, the advantage of a detailed study of the reorientational dynamics; the main reason is the lack of well-characterized optically anisotropic model systems.

Several investigations have been carried out in this direction, and in particular with stiff biological macromolecules, such as DNA,[5] tobacco mosaic virus,[6] and F-actin,[7] using static and dynamic light scattering. The self-diffusion of such systems in solution was also reported, using fluorescence photobleaching recovery (FPR).[8,9] However, although biological molecules are quite stiff, their inherent optical anisotropy is rather low; moreover, the presence of charges complicates the interpretation of data significantly. From the nonionic synthetic stiff polymers, the most extensively studied is poly(γ-benzyl α-L-glutamate), PBLG.[11,12] The results from the relevant studies are not fully conclusive concerning three aspects: (i) the mechanisms for relaxing concentration fluctuations in solution, especially in the concentrated region, where a coupling of translational to rotational diffusion is expected; (ii) the reorientational relaxation dynamics; (iii) the dependence of the self-diffusion on molecular parameters and concentration. On the other hand, investigations of the orientational dynamics, which are of primary interest in such anisotropic molecules were conducted more by electric birefringence and less by PCS experiments,[7,11,13−15] due to the small optical anisotropy of these systems, resulting in difficult, and sometimes ambiguous, measurements. Recent advances in macromolecular chemistry have led to the synthesis of well-defined poly(*p*-phenylenes), PPP, with aliphatic side chains, with varying molecular weights and much higher optical anisotropies compared to other molecules.[16,17]

Well-resolved measurements of orientational dynamics were subsequently carried out with PCS in semidilute solutions,[18] yielding two relaxation modes. These measurements, however, presented two complications:

First, and most importantly, PPP exhibits a dissolution problem as the concentration increases; it is due to clustering, despite the presence of side chains, whose role is solely to increase solubility. Thus, it is not clear to what extent these results reflect truly molecular properties and how the dynamics and kinetics of aggregation influence them. Second, it is evident from these studies that a complete understanding of the dynamics requires a systematic study of *both* VV and VH relaxations.

From the above, it is evident that there is a clear need for well-defined experiments with model systems, to resolve the present ambiguities and confusion related to the dynamics of rodlike polymers, e.g., the control of

* To whom correspondence should be addressed.
† Also at the Physics Department, University of Crete, 71110 Heraklion, Crete, Greece.

S0024-9297(97)01129-7 CCC: $15.00
Published on Web 02/07/1998

the aggregation process and the resolution of the various relaxation mechanisms. This will elucidate the effects of concentration, and provide the necessary ingredients for the assessment of the theoretical predictions. To address this challenge, we began an ambitious long-term systematic research program, ultimately aimed at investigating the potential pretransitional dynamics (near the isotropic-to-nematic transition) of hairy-rod PPPs. We have already determined accurately the conformation of these molecules by using depolarized Rayleigh scattering and magnetic birefringence[19] in dilute solution. Further, we have studied extensively the association dynamics in semidilute solutions using PCS, static light scattering, and SAXS;[20] we have in particular accounted for the effects of time and temperature. On the basis of our results, it is now clear that it is difficult to molecularly disperse these PPP solutions in toluene, but one can actually obtain well-defined small aggregates ("clusters", which actually are trimers on the average) even in dilute solution. Nevertheless, it is possible to control their growth with time, thus "effectively" isolate the aggregation process from the dynamics of nearly-molecular species.

This paper represents an extension of our previous investigations, by considering the dynamics of these hairy-rod polymers in the isotropic regime. Emphasis is given to the discrimination of molecular from aggregate processes using two different solvents, the effect of concentration, and the evaluation of the existing theoretical predictions. Section II reviews the theories on the dynamics of rodlike and semiflexible polymers in isotropic solutions. Section III describes the experimental procedure used, whereas the main findings are presented and discussed in section IV.

Finally, the conclusions from this work are summarized in section V.

II. Theoretical Background

A cage theory based on reptation arguments[1,15] and computer simulations[21,22] has attempted to elucidate the underlying mechanisms of translational and rotational mobilities and predict the dependence of the corresponding transport coefficients on the molecular length and concentration. The length L and the diameter b of a rodlike molecule define three concentration regimes in which the system, in principle, exhibits different dynamic behavior. The characteristic number concentrations $c^* = 1/L^3$ and $c^{**} = 1/(bL^2)$ define the dilute, semidilute, and concentrated regions. In the dilute region ($cL^3 < 1$), PCS probes single-molecule dynamics, and the isotropic dynamic structure factor $S_{iso}(q,t)$ and orientational correlation function $S_{or}(q,t)$ for short, relative to the scattering wavevector, molecules ($qL < 1$), are single exponential decay functions:[23]

$$S_{iso}(q,t) \propto N(\partial\pi/\partial c)^{-1}(\partial n/\partial c)^2 \exp[-q^2Dt] \qquad (1)$$

$$S_{or}(q,t) \propto N\beta^2 \exp[-(q^2D + 6D_r)t] \qquad (2)$$

$S_{iso}(q,t)$ is measured in the VV geometry, taking into account the anisotropic contribution, N is the number of scatterers in the scattering volume, $\partial\pi/\partial c$ is the osmotic modulus, $\partial n/\partial c$ is the refractive index increment, β^2 is the optical anisotropy of the scatterer, and D and D_r are the translational and the rotational diffusion coefficients, respectively. The diffusion coefficients, when extrapolated to zero concentration are $D_0 = D'F(L/b)$ and $D_{r,0} = D_r'F_r(L/b)$ for smooth rigid cylinders,[3,24] whereas for wormlike molecules they are $D_0^w = D'F_w(L/l)$ and $D_{r,0}^w = D_{r,0}F_{w,r}(L/l)$.[25,26] $D' = k_BT/3\pi\eta_sL$ and $D_r' = 3k_BT/\pi\eta_sL$,[3] with η_s being the solvent viscosity, F and F_r functions of the aspect ratio L/b, and F_w and $F_{w,r}$ functions of the contour length, L, the persistence length, l, and the diameter, b. When $c/c^* > 1$, the motion of each rod is expected to be hindered by its neighbors; however, experiments have shown that only above about $10c^*$ single molecule dynamics start to be affected.[2] As the concentration is increased beyond c^{**}, purely steric reasons can lead to an ordered mesophase, even in the absence of any other interactions, while the flexibility and polydispersity of the molecules can alter significantly the phase diagram of the system.[27]

At high concentrations, excluded volume effects, entanglement interactions, and hydrodynamic interactions affect the diffusion of the polymers. What is measured by dynamic light scattering is the cooperative diffusion coefficient, D_c, which represents the average response of a collection of macromolecules to concentration fluctuations. D_c is related to the osmotic modulus of the solution by[28]

$$D_c = \frac{M}{N_Af_c}(1-\phi)^2\left(\frac{\partial\pi}{\partial c}\right)_{T,P} \simeq D_o(1 + k_Dc + ...) \qquad (3)$$

where M is the polymer molecular weight, N_A is the Avogadro number, f_c is the cooperative friction coefficient, and ϕ the polymer volume fraction. The expression in the right-hand side of eq 3 is valid in the concentration range where the interactions are relatively small (virial regime), and only pair interactions between polymer chains are important; $k_D = 2A_2M_w - k_f - v_s$, with A_2 the second virial coefficient, k_f the effect of concentration on friction, and v_s the polymer specific volume. In this regime, D_c is predicted and found[5,12,29,30] to increase under good solvent conditions ($k_D > 0$).

The c dependence of the self-diffusion coefficients for solutions of rodlike and semistiff macromolecules is still under investigation, although there are numerous studies especially about the translational diffusivities. For infinitely thin rods in the semidilute region Doi–Edwards (DE) theory[1] based on the concept of undistorted cages and assuming that the normal diffusivity freezes ($D_\perp = 0$) and the parallel diffusivity is not hindered ($D_{||} = D_{||,0}$) predicts a decrease of the translational diffusion to half of its dilute value $D = {}^1/_zD_0$. Finite diameter effects were considered later,[31,33] predicting, in agreement with computer simulations,[22] a decrease of $D_{||}$ with c. Similar perturbation approaches[32] calculate the decrease of $D_\perp$ with c, predicting a more realistic, nonzero transversal diffusivity in the semidilure region. An extension of the above to consider the effect of flexibility was performed using the "fuzzy cylinder" model,[4,34] resulting in similar diffusion coefficients with rodlike molecules having renormalized dimensions (L_e, b_e). If the rodlike result $D_{||,0} = 2D_{\perp,0}$ is used as an approximation for a "fuzzy cylinder", we get

$$D_s = \frac{1}{2}D_0\left[(1 - a^{-1}L_e^2b_ec)^2 + \left(1 + \frac{B_\perp(b_e/L_e)L_e^3c}{(1 - a^{-1}L_e^2b_ec)}\right)^{-2}\right] \qquad (4)$$

where $B_\perp(b_e/L_e)$ is a correction factor and a is a constant.

Flexibility was also considered independently by Odijk,[35] Doi,[36] and Semenov,[37] who, on the basis of the reptation mechanism, predicted a c-independent D_s for concentrated solutions.

Another theoretical approach based on scaling ideas for semiflexible chains[8] predicts a strong decrease of D_s in the semidilute regime ($\sim l^{-5}L^{-2}c^{-3}$), while in the concentrated regime it is actually concentration independent. Experimental findings[8,30] so far reveal an almost linear decrease of D_s with c in the semidilute region, while in higher concentrations the decrease becomes even weaker, possibly indicating an approach to a c-independent translational diffusion.

While the rotational diffusion coefficient, D_r, initially predicted from the DE model[1] for rods in the semidilute region, was to exhibit a strong c dependence ($D_r/D_{r,0} \sim c^{-2}$), it is now evident, from both experimental studies[11,14,18] and other theoretical models and simulations,[21,15,22] that a rather weaker c dependence is followed until, only at high concentrations, the DE prediction is reached. These theories involve recalculation of the cage size[15] or consideration of dynamic distortion of cages and finite thickness effects.[4,21] On the other hand, the flexibility effects in the framework of the "fuzzy cylinder" model also give a weaker than c^{-2} dependence in the intermediate concentrations while at high concentrations D_r can decrease faster than c^{-2} due to the decrease of $D_{||}$:

$$D_r = D_{r,0}/\left[1 + \frac{B_r(b_e/L_e)cL_e^4/L}{(1 - B_{||}(b_e/L_e)L_e^3c)}\right]^2 \qquad (5)$$

where $B_r(b_e/L_e)$ and $B_{||}(b_e/L_e)$ are correction factors.[4] In a recent investigation of the rotational relaxation spectrum of a PPP,[18] we indicated the presence of two relaxation processes. The slow rate conformed to the c^{-2} DE prediction in the concentrated region, whereas the fast process displayed a weakly c-dependent rate and a c-dependent amplitude. The former was attributed to the rotation of the molecules through translation inside a cage, whereas the latter was attributed to a faster tumbling motion of the smaller molecules inside the cage.

The coupling between isotropic concentration and orientational fluctuations in stiff polymer solutions can affect the shape of $C_{VV}(q,t)$ and $C_{VH}(q,t)$ correlation functions. The dynamic isotropic light-scattering spectrum of an isotropic solution of rigid rods was considered by Doi, Shimada, and Okano (DSO)[38] using mean-field theory, to account for the translation−rotation coupling of the rod diffusion, the excluded volume interactions, the entanglement effects, and the hydrodynamic interactions. Later, Maeda reformulated the DSO theory to calculate both the isotropic and VH correlation functions[39] in the whole q and t regime. In the low-q limit, these theories predict a double exponential decay for $C_{iso}(q,t)$[38] and a much more complex shape for $C_{VH}(q,t)$;[39] the latter becomes identical to the Zero−Pecora expression[11] at the limit of low c's and q's. The two relaxation modes of the concentration fluctuations are attributed to the coupling with orientation fluctuations, which becomes more important as the system approaches the isotropic to nematic transition. The fast mode relates to the relaxation of concentration fluctuations, preserving the orientation, and both intensity and rate increase with concentration; an increase of concentration favors the regions with enhanced orientation, where concentration fluctuations relax predominantly through axial diffusion. The slow mode is related to the relaxation of concentration fluctuations which involves changes of orientation of rods and hence becomes slower and weaker with increasing concentration as orientational changes become less favored.[3]

Table 1. Molecular Characteristics of the Poly(*p*-phenylene) Samples

sample	M_n	L_n (nm)	L_w/L_n	L_e (nm)
PPP-2	9 900	25.7	3.2	22.3
PPP-3	12 600	32.6	3.1	27.3
PPP-5	14 800	38.5	3.2	31.4

III. Experimental Section

Materials. The synthesis of hairy-rod poly(*p*-phenylenes), PPPs, with dodecyl side chains (the hairs) has been reported elsewhere.[16,17] In the present work, a series of PPPs with slightly different molecular weights was utilized. The molecular characteristics are summarized in Table 1 (L is the contour length, whereas the subscripts w, n, and e refer to weight average, number average, and "effective", respectively). These specific molecules were chosen because of their large optical anisotropy, originating from the highly conjugated phennylene backbone. As already mentioned in the Introduction, the flexible side chains were introduced to improve solubility, since it is known that poly(*p*-phenylenes) without side chains are only soluble in strong acids.[2] Due to the synthesis method used (polycondensation), PPPs are rather polydisperse, as can be seen in Table 1. Depolarized Rayleigh scattering measurements were carried out in order to determine the persistence length (l) by utilizing the wormlike model and taking into account the polydispersity; l was found to be about 28 nm.[19] The investigation of the aggregation behavior of these molecules in two different organic solvents (toluene and chloroform) has led to the distinction of the molecular ("trimer" in the case of toluene) and aggregate contribution to the polarized light-scattering spectrum.[20]

Solutions were prepared by dissolving the appropriate amount of PPP in spectroscopic grade solvent (toluene or chloroform), under continuous stirring overnight, at concentrations below 4 mg/cm^3. Dust-free samples were subsequently obtained by careful filtration of the dilute solutions through a 0.22 μm Teflon Millipore filter into a dust-free light-scattering cell (diameter 10 mm). Higher concentrations were obtained by slow evaporation. The solutions were measured at 25 °C, after heating at high temperatures overnight (80 °C for toluene solutions and 60 °C for solutions in chloroform), to avoid aggregation after a few days.[20] The overlap concentration, c^*, for rigid rods is estimated from an effective contour length L_e, equal to the end-to-end distance of the polymer chain. The latter is calculated in the framework of the wormlike model using the number average contour length, L_n, and $l = 28$ nm. It is finally noted that due to the high polydispersity and small range of molecular weights of the polymers of Table 1, it is not possible to examine the effects of molecular weight unambiguously.

Photon Correlation Spectroscopy (PCS). The autocorrelation function, $G(q,t) = \langle I(q,t)\, I(q,0)\rangle/\langle |I(q,0)|\rangle^2$, of the polarized or depolarized light-scattering intensity, $I(q,t)$, at a scattering wavevector $q = (4\pi n/\lambda)\sin(\theta/2)$ (n is the refractive index of the medium, λ is the wave-

length of the incident beam, and θ is the scattering angle),[23] was measured with an automated ALV goniometer and an ALV-5000 full digital correlator (320 channels) over the time range 10^{-7} to 10^{3} s. The light source was a Nd:YAG dye-pumped, air-cooled laser (Adlas DPY 325) with a single mode intensity of 100 mW, and $\lambda = 532$ nm. The measured homodyne normalized light-scattering intensity autocorrelation function $G(q,t)$ is given by the Siegert relation:

$$G(q,t) = 1 + f^*|\alpha C(q,t)|^2 \tag{6}$$

where f^* is an experimental instrument factor (which relates the scattering area to the coherence area) calculated by means of a standard, α is the fraction of the total scattered intensity arising from fluctuations with correlation times longer than 10^{-7} s), and $C(q,t)$ is the normalized field correlation function:

$$C(q,t) = \frac{\langle E(q,0)\, E(q,t)\rangle}{\langle |E(q,0)|^2\rangle} \tag{7}$$

where $E(q,t)$ stands for the scattered electric field.[23]

During the accumulation time, the light-scattering intensity remained constant. Two procedures were chosen for the analysis of the experimental correlation functions, $C(q,t)$.

(i) Inverse Laplace transformation (ILT), using the program CONTIN.[40] This method assumes that $C(q,t)$ can be represented by a superposition of exponentials:

$$\alpha C(q,t) = \int L(\ln \tau) \exp(-t/\tau)\, \mathrm{d}(\ln \tau) \tag{8}$$

which determines a continuous spectrum of relaxation times $L(\ln \tau)$. The characteristic relaxation times, τ, correspond to the maximum values of $L(\ln \tau)$. A typical VV field autocorrelation function in the dilute and semidilute regimes, at $\theta = 150°$, is shown in Figures 1a,b, respectively (for PPP-5, $c = 3$ mg/cm^3 and $c/c^* = 3.8$, in toluene, and $c = 2.9$ mg/cm^3 and $c/c^* = 3.5$, in chloroform).

(ii) The nonexponentiality of $C(q,t)$ can be described by the Kohlrausch−Williams−Watts (KWW) function:

$$C(q,t) = \exp[(-t/\tau)^{\beta}] \tag{9}$$

where β is the shape parameter ($\beta = 1$ corresponds to a single exponential relaxation process).

Pulsed Field Gradient (PFG)-NMR. This technique measures essentially a stimulated echo using a proton spin as a probe, yielding the translational diffusion coefficient, D_s, of particles bearing ^{1}H nuclei, if the field gradient is applied as a pulse during the spin-echo experiment.[41] A magnetic gradient pulse of magnitude g is applied for a dephasing period δ, and the echo amplitude $\Psi(q,t)$ is measured during the time interval, t, between the field gradient pulses. The height (g) and the width (δ) of the field gradient pulses define the generalized wavevector $q = \gamma g \delta$, with γ being the gyromagnetic ratio; q may be varied via either the gradient amplitude g or the pulse duration δ. However, switching the gradient on and off does not permit the reduction of δ below about 10^{-3} s. Large q values require strong magnetic field gradients and are limited by thermal and mechanical problems with the large currents in the field gradient coil.

The range of q in the present experiments extends up to about 10^{-2} nm^{-1}. On the other hand, the longest accessible diffusion times are determined by the spin−lattice relaxation time T_1, which is of the order of seconds; t may be varied between 10^{-3} s and T_1.

IV. Results and Discussion

A. General Features. As already discussed, for solutions of rodlike polymers c^* is very small, and thus PCS measurements in the dilute regime are difficult. In fact, the lowest concentration studied in this work ($c = 0.6$ mg/cm^3 for PPP-2 in toluene) was determined by the ability of the PCS technique to resolve good VV correlation functions within a few hours. For rods with significant flexibility, c^* can be estimated either from the R_g of the polymer chain or from its end-to-end distance. In the former case, $c^* = (4\pi R_g^3/3)^{-1}$ and the macromolecule assumes a coil conformation, which can be true for chains with contour length much higher than their persistence length. On the other hand, molecules with contour lengths close to the persistence length, like the present PPPs, resemble a bent rod, which is characterized by an end-to-end distance, $L_e = \langle R^2\rangle^{1/2}$, and an effective diameter, b_e, larger than the molecular diameter b.[34] In such a case, the overlap concentration can be approximated by $c^* = 1/L_e^3$. The corresponding c^* values, for these PPP molecules, are about 10 times smaller than those based on R_g. It is noted that extending the measurements to $c \gg c^*$ was precluded by the limited solubility of the present polymers. At relatively low concentrations (less than 10 wt %) solutions of these hairy-rod polymers in both toluene and chloroform undergo a transition, which is characterized by the formation of large clusters, eventually settling with time (if the polymer−solvent density difference allows). This phenomenon was found to relate to association, driven by van der Waals forces, and a subsequent crystallization of the flexible side chains inside the clusters.[20] As a general observation, nondilute solutions of these PPPs in both toluene and chloroform eventually phase separate, at similar concentrations (~55 mg/cm^3).

The static intensity as well as the dynamics in the low-concentration regime can be used to extract information about the molecular characteristics of the scatterers due to negligible interactions. The scattered intensity, extrapolated to zero c and q, yields the M_w, the R_g, and the second virial coefficient A_2. Solutions in toluene revealed bad solvent conditions, as A_2 was found to be negative (typically $A_2 \simeq -6 \times 10^{-4}$ cm^3/g^2), whereas solutions in chloroform exhibited good solvent behavior (typically, $A_2 \simeq 1 \times 10^{-3}$ cm^3/g.[2] In toluene, the molecular weight of PPP-2 was found to be significantly higher than in chloroform, in agreement with the values of the translational diffusion coefficient at $c \rightarrow 0$, D_0. Based on the values of M_w and D_0 in both solvents, we can conclude that small clusters (aggregates), consisting on the average of three chains, are formed in toluene, even in dilute solution,[20] whereas association is negligible in chloroform, at low concentrations.

B. Cooperative Diffusion. In the dilute regime, a single translational diffusion process can be detected, irrespectively of the solvent quality.

However, this relaxation process is rather broad. In the KWW analysis (eq 9), β typically varies between 0.7 and 0.9, for concentrations up to about 5 mg/cm^3; this may be attributed to the large polydispersity of the samples (see Table 1). The $C(q,t)$ of Figure 1a in the dilute regime is a single diffusive relaxation, as also

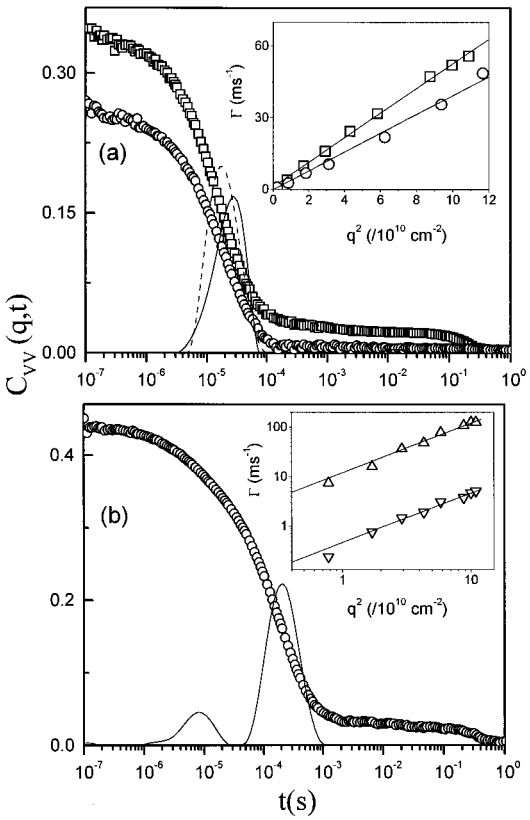

Figure 1. (a) Net polarized field autocorrelation functions $C_{VV}(q,t)$ (eq 7) for dilute solutions of PPP-5 in toluene (c = 3 mg/cm^3; ○) and chloroform (c = 2.9 mg/cm^3; □) at 25 °C and a scattering angle $\theta = 150°$ ($q \simeq 0.034$ nm^{-1}), along with their corresponding distributions of relaxation times, obtained from ILT analysis (eq 8; solid and dashed lines, respectively). Inset: q^2 dependence of the corresponding decay rates, Γ. (b) Net normalized polarized field autocorrelation function for a 41.4 mg/cm^3 solution of PPP-5 in chloroform (○), along with the respective ILT distribution of relaxation times. Inset: q^2 dependence of the corresponding two decay rates, fast (△) and slow (▽). The ultraslow mode, apparently due to dust or "cluster processes", was not considered in the fitting and analysis of the correlation function. The corresponding data are consistent at all concentrations and solvents.

confirmed by the relaxation spectrum $L(\ln \tau)$, eq 8, shown in this figure as well, and the q^2 dependence of the decay rate, Γ (inset of Figure 1a); it is attributed to the translational diffusion of the PPPs. As the concentration increases above about 8 mg/cm^3, the VV correlation function becomes broader for both solvents. Moreover, for chloroform solutions, two relaxation modes can be resolved by the ILT analysis. In Figure 1b, the $C(q,t)$ of a semidilute chloroform solution of PPP-5 (c = 41.4 mg/cm^3, c/c^* = 50.2) at $\theta = 150°$ ($q = 0.033$ nm^{-1}) clearly reveals these two relaxation modes, which are both diffusive (inset of Figure 1b). While the fast process is identified with the cooperative diffusion, on the basis of the c dependence of the diffusion coefficient and the scattered intensity, the slow mode's origin will be discussed in the next section.

The (weak) q dependence of the scattered intensity can lead to an (approximate) estimation of the correlation length ξ. If we use the total scattering intensity, ξ is found to be nearly independent of concentration, about 15 nm, for all samples; actually, it is expected to drop from its dilute region value, where it represents the geometric characteristics of the macromolecule (R_g), to some average mesh size of the network formed by

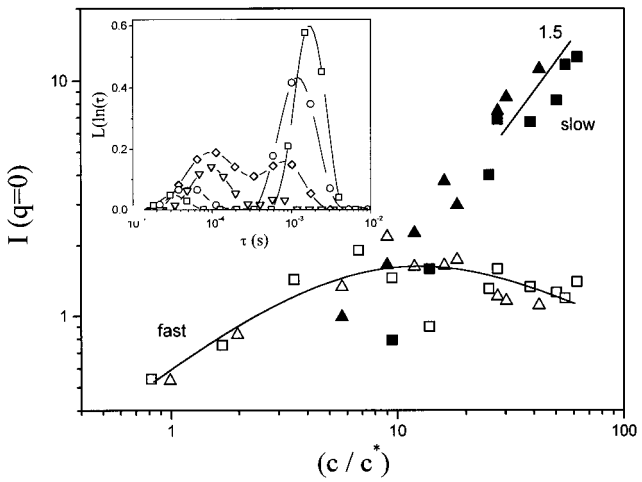

Figure 2. Concentration dependence of the light-scattering intensities of the two dynamic modes, extrapolated to $q \rightarrow 0$ and normalized with the polarized toluene intensity, for two PPP samples (squares, PPP-2; triangles, PPP-5). Open and solid symbols correspond to the cooperative and slow modes, respectively. Lines are drawn to guide the eye or indicate slopes. Inset: Distribution of relaxation times (eq 8), for PPP-2 in chloroform at $\theta = 45°$ ($q = 0.014$ nm^{-1}) and four concentrations: $c/c^* = 0.99$ (▽); 9.01 (◇), 30.3 (○), 42.1 (□).

the overlapping polymer chains in the semidilute region. In solutions of flexible polymers, $\xi \sim c^{-3/4}$,[42] whereas for rods it is expected to drop, as the transition to the nematic state (at c_n) is approached, as $\xi \sim (1 + 8c/c_n)^{-1/2}$, according to the Onsager theory[26] and mean-field predictions.[38] A weaker decrease, compared to that of flexible molecules in solution, has been observed and predicted for wormlike chains,[4,43] but an even weaker decrease than the predicted $c^{-1/2}$ has been found[12] in solutions of stiff macromolecules. Nevertheless, the c dependence of ξ represents a still unresolved issue, since the total scattering intensity includes several contributions. It is noted that in our study, the intensity of the cooperative diffusive process ($q\xi \ll 1$), I_c, is virtually q-independent, whereas the intensity of the slow process, I_s, increases weakly at low q's and becomes q-independent at even higher c's.

Figure 2 depicts the concentration dependence of the scattered intensities and the distribution of relaxation times $L(\ln \tau)$ of PPP solutions in chloroform. The scattered intensities $I(q \rightarrow 0)$ are shown for PPP-2 and PPP-5 solutions. The concentration is normalized with c^* and the intensity of each mode is calculated from its relative contribution to the correlation function and the total scattering intensity, I, relative to toluene, i.e., $I_i = a_i I$. It is noted here that the PCS technique offers the unique advantage of isolating various contributions (such as slow modes) from the total scattering intensity, and thus accurately determining parameters such as osmotic modulus and friction coefficients, and of course identifying the characteristics of relaxation modes other than the cooperative diffusion. The intensity I_c associated with the cooperative diffusion mode increases with concentration only in the dilute regime, whereas this increase ceases as intermolecular interactions become significant, signifying the transition to the semidilute regime. The broad peak of I_c versus c occurs around $c \approx 10c^*$; above this concentration, negative interference leads to the decrease of I_c. This rather extended transition is common in rodlike polymer solutions, where the onset of the semidilute region occurs at c/c^*

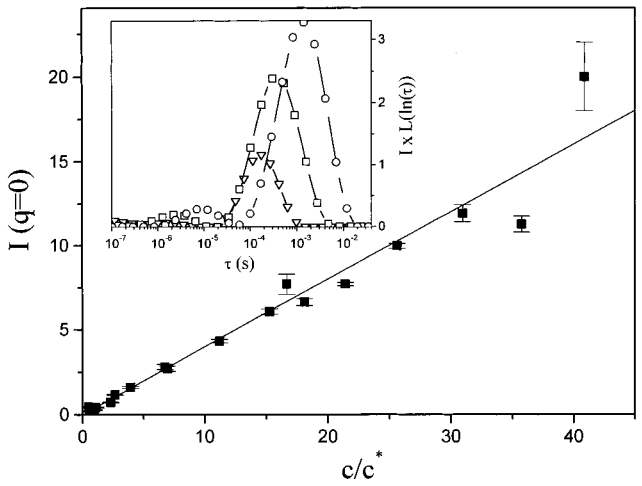

Figure 3. Concentration dependence of the light-scattering intensity for PPP-2 in toluene (■). The solid line represents the linear fit. Inset: Corresponding distribution of relaxation times $L(\ln \tau)$ (eq 8), at $q = 0.014$ nm^{-1} and various concentrations: $c/c^* = 6.8$ (▽), 21.4 (□), 40.9 (○). $L(\ln \tau)$ are multiplied by the total polarized intensity I for comparison reasons. The fitting procedure (eq 8) can resolve fast low-intensity modes as well (see text).

$\approx O(10)^{2,3}$ and not at $c \approx c^*$; this difference matches the disparity between the volumes L^3 and $^4/_3\pi R_g^3$ for rods and flexible coils, respectively. For $c > 10c^*$, I_c decreases weakly, whereas the intensity I_s associated with the slow mode increases strongly, with concentration; this is also evident from the distribution of relaxation times, $L(\ln \tau)$, of PPP-2 solutions in chloroform, shown in the inset of Figure 2, at $\theta = 45°$ ($q = 0.014$ nm^{-1}). It is noted that for $c \approx 10\ c^*$ the separation of the two processes is not sufficient, and hence the intensities are subject to larger error. However, the mode resolution increases with c since the two diffusion coefficients have opposite c dependence.

To confirm the ability to resolve relaxation modes of molecular origin, we performed measurements in a solvent of reduced quality, i.e., toluene. In such a case, one main relaxation process that is related to isotropic fluctuations is unambiguously detected in the VV correlation function. Like in chloroform solutions, this mode is clearly diffusive, and for all samples it is slower than the cooperative diffusion process in chloroform. In contrast to the latter, the diffusion coefficient in toluene is decreasing with concentration for the PPPs. Moreover, the intensity $I(q=0)$ increases monotonically with c, in contrast to the behavior of I_c in chloroform, and hence the signature of the crossover to the semidilute regime is unclear for the toluene solutions. The reference value of c^* used for solutions in toluene is the same as that for chloroform solutions. The concentration dependence of I of PPP-2 solutions in toluene is depicted in Figure 3. On the other hand, the distribution of relaxation times, shown in the inset of Figure 3 for different concentrations at $q = 0.014$ nm^{-1}, suggests that at least one faster process with relatively low-intensity is present in toluene solutions; this could relate to cooperative diffusion, but it is overwhelmed by the slow mode. On the basis of the comparison between this fast process and the depolarized correlation function (section IV.D), the former originates from orientation rather than concentration fluctuations. The different behavior of both the intensity and the dynamics of the main mode in toluene solutions, as compared to the cooperative diffusion in chloroform (Figure 2), suggests

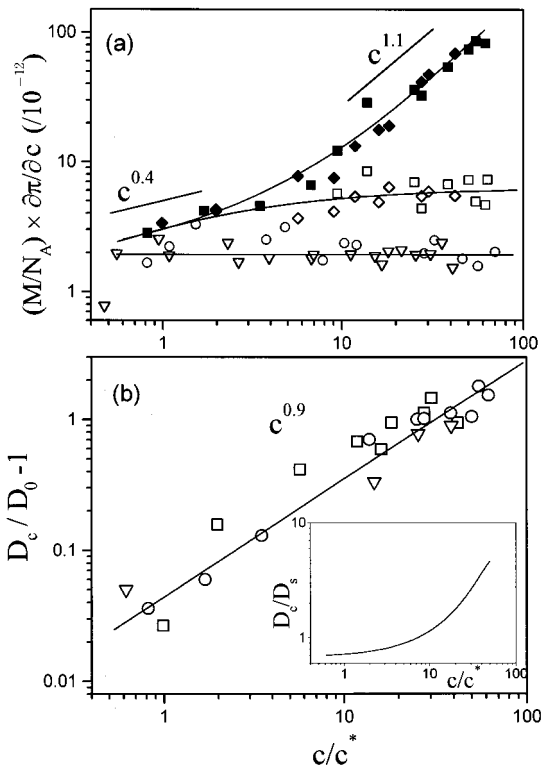

Figure 4. (a) Concentration dependence of the osmotic modulus (normalized with molecular weight), as deduced from the cooperative and total intensities, for PPPs in two solvents: chloroform [(cooperative) PPP-2 (◆) and PPP-5 (■); (total) PPP-2 (◇) and PPP-5 (□)] and toluene [(total) PPP-2 (▽) and PPP-5 (○)]. Solid lines are drawn to guide the eye or indicate slopes. (b) Concentration dependence of the cooperative diffusion coefficient (normalized with D_0) in chloroform: PPP-2 (□); PPP-3 (▽); PPP-5 (○). The solid line represents the linear fit with slope 0.9. Inset: Concentration dependence of D_c/D_s.

that the origin of this mode is not the mutual diffusion of the polymer chains in semidilute solution. As will be discussed below, this slow process is related to the self-diffusion of small aggregates.

Figure 4a depicts the osmotic modulus, $\partial\pi/\partial c$, reduced by the molecular weight, for solutions of PPP-2 and PPP-5 in both solvents; it can be calculated either from the total scattered intensity or from the intensity I_c of the cooperative mode (in the case of chloroform solutions); we recall that the average total intensity includes contributions from the slow mode as well. The osmotic modulus represents the resistance of the polymer solution to concentration fluctuations and is expected to increase with concentration, suppressing the scattered intensity. In chloroform, total scattering intensity data lead to a small increase of $\partial\pi/\partial c$ at low concentrations and a final level-off for $c/c^* \gtrsim 7$. Over the examined concentration range, solutions in toluene reveal a practically constant osmotic modulus, being about 3 times smaller than in chloroform. This finding corroborates the notion that there are more aggregates (trimers) in toluene than in chloroform, manifested also in the VH dynamics (section IV.D). The presence of an additional slow process, however, can strongly alter the values and the c dependence of the osmotic pressure. The latter $\partial\pi/\partial c$ based on I_c, clearly reveals the expected behavior for all samples used (PPP-2 and PPP-5, Figure 4a). In the semidilute region ($c > 10c^*$) $(M_w/N_A)(\partial\pi/\partial c) \sim c^{1.1\pm0.1}$, whereas in the virial regime ($c < 10c^*$) the

dependence is weaker ($\sim c^{0.4}$) (Figure 4a). The mean-field prediction[38] for $\partial\pi/\partial c$ of rodlike polymer solutions is a linear increase with c, $(M/RT)(\partial\pi/\partial c) = 1 + 8c/c_n$, while scaling particle theory for wormlike chains predicts, at high concentrations, a stronger than c^2 dependence.[4,43] For comparison, in semidilute solutions of flexible linear chains $\partial\pi/\partial c$ scales with $c^{1.3}$.[42] In the present investigation, neither ξ nor $\partial\pi/\partial c$, deduced from total intensity data, exhibits the standard behavior of a rodlike solution (Figure 4a). A linear c dependence for $\partial\pi/\partial c$ over the whole c range, would assume the slope of 1.7 ± 0.3, which in the light of the DSO theory would suggest that $c_n \approx 4c^*$. However, this could not be verified, since the present PPPs phase separate before they form a nematic phase; moreover, it is not consistent with the behavior of D_c. The osmotic moduli of solutions of these semiflexible PPPs in the semidilute regime exhibit therefore a behavior intermediate between rigid-rod and flexible homopolymers. The weaker, compared to that of the flexible polymers, increase of $\partial\pi/\partial c$ can be rationalized by the fact that a semistiff chain has a much more looser structure than a flexible coil, facilitating interparticle mixing in the semidilute and concentrated regimes. Experiments on PBLG and xanthan solutions have indicated that $\partial\pi/\partial c \sim c^1$.[12,29] In the other extreme of reduced interparticle mixing, a sharp osmotic modulus increase with concentration is reported for multiarm star polymers and hard colloidal particles.[44,45]

The speed-up of D_c above c^*, shown in Figure 4b, is due to increasing intermolecular interactions and excluded volume effects, which surpass the increase of the friction with concentration. It is worth mentioning that in semidilute solutions of flexible polymers, it is the reduction of the blob size that is responsible for the increase of D_c with c. In the case of rodlike polymers, all the segments are correlated, moving in phase, and thus the motion of a part similar in size with the correlation length follows the motion of the whole molecule. In the wormlike molecular picture, the statistical segment is twice the persistence length and hence molecules with $L \simeq 2l$ should move in a more correlated fashion, compared to flexible chains, even in concentrated solutions. DSO theory predicts that $D_c = (D_0/2)[1 + 8c/c_n]$ varies linearly with c, assuming that the self-diffusion coefficients behave according to the DE theory[1] ($D_{||} = D_{||,0}$, $D_\perp = 0$). From Figure 4b it can be seen that $D_c/D_0 - 1$ scales with $(c/c^*)^{0.9}$, which implies that $c_n \approx 100c^*$. This is certainly an overestimation and a contradiction with the estimation of c_n based on the comparison of $\partial\pi/\partial c$ data with DSO predictions. We therefore conclude that DSO predictions do not conform with our experimental findings.

In the virial regime, D_c (eq 3) should vary linearly with c (assuming that higher order terms are negligible) and its slope should yield k_D. In chloroform solutions, k_D is found to be positive, in qualitative agreement with the static light-scattering result; i.e., chloroform is a good solvent for these PPPs. In this regime, the experimental data yield $k_D = 39$ cm^3/g for PPP-5. The calculated value of $k_D = 2A_2M_n$, neglecting the effects of friction and excluded volume and using the experimental A_2 value for PPP-5, is 36 cm^3/g. The computed value is significantly larger (129 cm^3/g), if the Ishihara–Hayashida[46] expression $A_2 = \pi f N_A d^2 L_n/M_n^2$ is used. For solutions in toluene, k_D is expected to be negative, since both the thermodynamic ($A_2 < 0$) and friction factors slow the diffusion. This is in qualitative agreement with

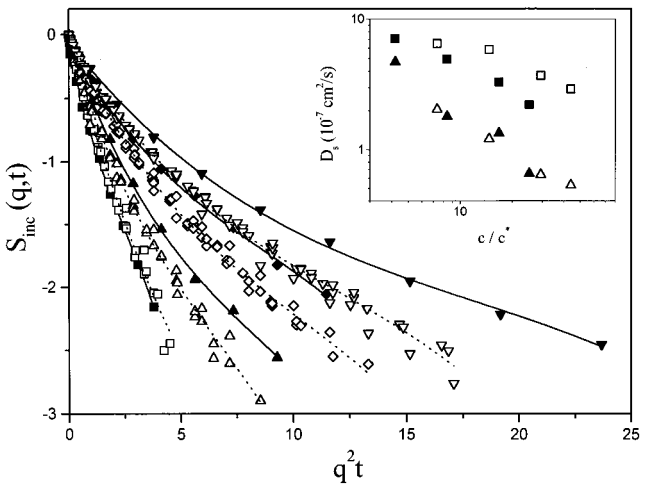

Figure 5. Incoherent structure factor, $S_{inc}(q,t)$ of the pulsed field gradient NMR experiment on various PPP-3 solutions in two solvents. Open sympols represent measurements in chloroform at concentrations (going up) 7.5, 15, 30, and 45 mg/cm^3, respectively. Solid symbols refer to PPP-3 solutions in toluene at concentrations (going up) 4.34, 8.67, 17.3, and 26 mg/cm^3, respectively. Solid and dashed lines represent cumulant fits (see text). Inset: Concentration dependence of the self-diffusion coefficients: short-time, (□ and ■); long-time (△ and ▲).

experiments, since there is no relaxation mode with increasing decay rate in toluene solutions.

C. Slow Mode: Self-Diffusion. The slow mode appears in chloroform solutions in the semidilute regime, whereas in toluene it is always dominant, overwhelming the cooperative diffusion (Figures 1−3). From the increase of the intensity with concentration, it is clear that this mode is not related with the slow mode of the DSO model of isotropic solutions of rodlike molecules in the vicinity of the nematic transition.[12] The diffusion coefficients D_s related to the slow mode in chloroform, or the main one in toluene, decrease with concentration (Figure 6 below). Slow modes were found in several dynamic investigations of both stiff and flexible polymer solutions, and in most cases they were attributed to clusters.[5,9,47] In a few light-scattering experiments slow modes were related to the self-diffusion of the scatterers.[6,48,49] However, an independent experimental verification was missing. For polydisperse particles, it has been predicted theoretically that not only concentration fluctuations (relaxing through collective motions) give rise to refractive index variations but also exchange fluctuations from particles of different refractive index or/and size, enabling thus the observation of the self-diffusion of the molecules by dynamic light scattering; this has been observed in different systems: colloidal spheres and rods,[6,50] multiarm star polymers,[44] and block copolymers.[51] For rods that are polydisperse in size, the dynamic structure factor is predicted to split into two terms:[6]

$$C_{VV}(q,t) = A_c \exp^{-q^2D_ct} + A_s \exp^{-q^2D_st} \qquad (10)$$

where A_c and A_s are the amplitudes.

To find the origin of the slow mode, we also carried out PFG-NMR measurements, probing directly D_s, for PPP-3 at different concentrations, as seen in Figure 5. The same procedure as in PCS measurements was used, in order to prevent clustering. A third cumulant

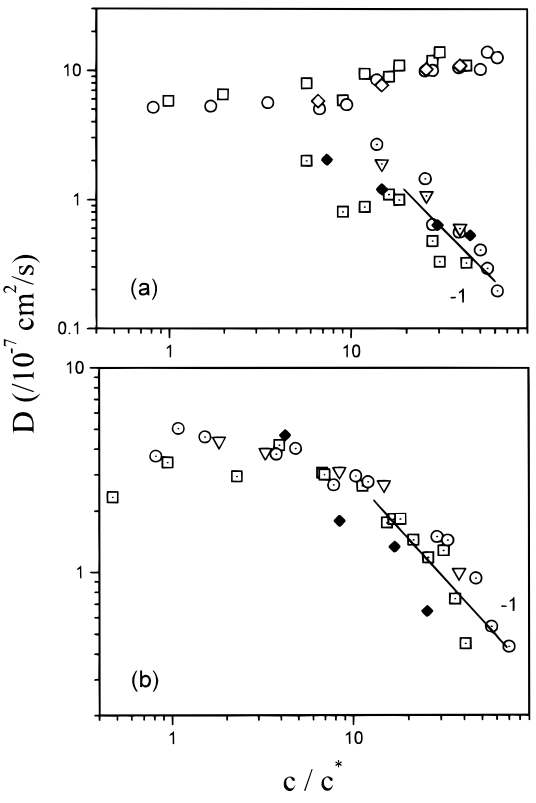

Figure 6. Concentration dependence of the diffusion coefficients obtained from polarized dynamic light scattering for all samples in chloroform (a) and toluene (b). PPP-2: (□) cooperative mode; (⊡) slow mode (both solvents). PPP-3: (◇) cooperative mode; (▽) slow mode (both solvents). PPP-5: (○) cooperative mode; (⊙) slow mode (both solvents). The long-time self-diffusion coefficient for PPP-3 solutions in both solvents (◆) is also shown for comparison.

analysis fit[52] was chosen for the incoherent structure factors:

$$\ln (S_{inc}) = A - \overline{D_s} q^2 t + {}^1/_2 \mu_2 (q^2 t)^2 - {}^1/_6 \mu_3 (q^2 t)^3 \quad (11)$$

where A is the amplitude, $\bar{D}_s = \bar{\Gamma}/q^2$ is the diffusion coefficient related to the initial decay rate, and $\mu_2 \equiv \int (\Gamma - \bar{\Gamma}) G(\Gamma)\, d\Gamma$ and $\mu_3 \equiv \int (\Gamma - \bar{\Gamma})^2 G(\Gamma)\, d\Gamma$ are the second and third moments of the decay rate distribution $G(\Gamma)$, respectively. A measure of the breadth of the distribution is the ratio $\mu_2/\bar{\Gamma}^2$ ($\equiv [(\bar{D}^2)_z - (\bar{D}_z)^2]/(\bar{D}_z)^2$, the z-average normalized variance of the D distribution); in toluene, it increases with c from 0.18 to 0.4. For nearly the same concentrations in the two solvents, the tail of the distribution is more pronounced in toluene, resulting in a larger $\mu_2/\bar{\Gamma}^2$. For the highest concentrations, the third distribution is found to be important as well ($\mu_3/\bar{\Gamma}^3 \simeq 0.12$ for the larger concentration in toluene). Therefore, we also estimated the long-time diffusion from the slope of $\ln(S_{inc})$ at long times. From these data, it is clear that D_s decreases with c, as seen in the inset of Figure 5. Furthermore, the characteristic times of the long-time decay are essentially the same in both solvents, whereas for the short-time decay, the times in toluene are slower, the difference being larger at higher concentrations.

The PFG-NMR D_s data, obtained from the long-time decay, compare favorably with the slow diffusion PCS data for chloroform, or the main diffusion for toluene. A compilation of all diffusion coefficients is presented in Figure 6, for all samples and concentrations investigated. In the case of chloroform (Figure 6a), the dramatic difference of cooperative and slow diffusion coefficients is a manifestation of the different origins of these two mechanisms of relaxation of isotropic fluctuations; moreover, it confirms the assignment of the slow mode detected by PCS to self-diffusion, in both solvents (see also Figure 6b). It appears that the slow mode seen in light scattering and the long-time diffusion measured by PFG-NMR originate from the self-diffusion of small clusters in the solution of the single polymer chains. In addition, PFG-NMR also measures the self-diffusion of single molecules, which is represented by the initial decay or first cummulant diffusion coefficient ($\bar{D}_s$) and, as expected, is faster than the self-diffusion of clusters but decreases with a similar rate. The reason for detecting with PCS the motion of individual clusters, and thus their self-diffusion, is the refractive index and size difference that they have relative to single molecules in solution. The former can well be the result of the higher local concentration of polymers inside a cluster. This justifies the necessary optical contrast for scattering of light due to spatial composition fluctuations, which relax through the self-diffusion of the clusters. It is clear, however, from the dynamics and the q dependence of the intensity, that we do not have large clusters in the solution, even in toluene, such as the ones investigated recently.[20] It is noted that the system is in equilibrium during the time of the measurements and that both the dynamic and static results were in all cases reproducible.

It is further noted that on the basis of the excellent agreement between light scattering and PFG-MNR data (Figure 6), as well as knowledge of the system under study[20] and the rather low nominal concentration of the polymer, we can justify the ability of photon correlation spectroscopy to determine self-diffusion (which requires for the current case that the clusters be dilute). From another point of view, the situation resembles the interdiffusion in a ternary mixture of two homopolymers and a solvent where the refractive index difference between the two species results in the observation of the diffusion of one species relative to the other.[53]

The intensity of the slow mode in chloroform is shown in Figure 2; it scales with $c^{1.5}$. In toluene, the total scattering intensity, which increases almost linearly with c, is probably a result of two opposing factors, the increase of the slow mode intensity and the decrease of that of the cooperative mode; this is also the case for the total intensity in solutions of chloroform. In both solvents, at the high concentrations, $D_{slow} \sim c^{-1}$, within experimental error (Figure 6); the scattering of the data is attributed in part to the slight difference in molecular weights between samples, as seen in Table 1. The slowing down of the dynamics is not accompanied with an increase of ξ, which, as already mentioned, is found to be nearly c-independent. These findings suggest that the origin of the slow mode is molecular associates that do not increase in size. Further, in chloroform, the scatterers do not increase in size with c, but rather they increase in number. It appears that, although we cannot separate the scattering intensity of the slow mode in toluene, this should have a behavior similar to the one in chloroform, i.e., faster than linear increase, which is due to the increasing number of clusters formed, while their size remains constant. Further, a comparison of $\partial\pi/\partial c$ (calculated from the total I) in

connection with the similar ξ'*s* found in the two solvents, suggests that the clusters, which represent the main contribution to I at higher concentrations, are about 3 times more numerous in toluene than in chloroform. Moreover, the practically same size explains the similarity of the long-time diffusion and slow diffusive mode in the two solvents.

As discussed above, the self-diffusion of the single molecules is represented by the initial decay of the incoherent structure factor measured in PFG-NMR. This scales with $c^{-0.5}$ in both solvents, within experimental error. The c dependence of D_s of the polymer chains is smaller than that predicted theoretically (see section II); the scaling ideas by Tinland et al.[8] in the semidilute regime ($D_s \sim c^{-3}$) and the "fuzzy cylinder" approach (eq 4) in the high-concentration limit predict a much sharper decrease of D_s. Nevertheless, at intermediate concentrations, the latter theory predicts a weaker decrease of D_s (eq 4), relating the c-independent dilute regime with the high-c regime. This is in qualitative aggreement with the experimental data; a quantitative comparison with theoretical predictions requires measurements in an extended concentration region.[54]

The self-diffusion from PFG-NMR can also be used along with the cooperative diffusion of the single polymer chains from PCS to assess the relation of f_s and f_c, the self-friction and mutual friction coefficients, respectively, since $D_c/D_s = (\partial\pi/\partial c)f_s/f_c$. The self-friction is related to the motion of a single particle, whereas the mutual friction represents the resistance of the solution to a concentration gradient imposed by thermal fluctuations. In the inset of Figure 4b, the ratio D_c/D_s is shown for PPP-3. By comparing D_c/D_s with $(M_w/N_A)(\partial\pi/\partial c)$, shown in Figure 4a, we see that $\partial\pi/\partial c$ determined directly from the scattering intensity of the cooperative mode increases faster with c than the ratio D_c/D_s. This means that $f_s/f_c < 1$: the mutual friction coefficient is larger than the self-friction. This behavior relates to the negative velocity cross-correlation of polymer chains in a semidilute solution, which can be visualized as movement of the polymer chains away from each other in an effort to relax concentration fluctuations. This has been found also in PBLG solutions for a similar concentration regime, whereas for higher concentrations an opposite relation ($f_s/f_c > 1$) has been found.[10]

D. Rotational Diffusion. Orientational dynamics are observed mainly in toluene solutions, whereas for similar concentrations in chloroform the relaxation times of the orientation fluctuations are too fast to be detected in the PCS time window. The VV measurements in toluene in dilute and semidilute solutions revealed one main diffusion process, associated with the self-diffusion of the clusters, as already mentioned (Figures 1a and 3). For $c > 25$ mg/cm^3, well into the semidilute regime, a faster relaxation process is also detected (inset of Figure 3); it can be better resolved at low scattering angles due to its q-independent decay rate, in contrast to the diffusive main mode. Figure 7 demonstrates the existence of this fast process unambiguously, for PPP-5 at $c = 36.9$ mg/cm^3 ($c/c^* = 46.3$) and $q = 0.009$nm^{-1}. This nondiffusive mode is attributed to the rotational dynamics of the scatterers (trimers), through the contribution of I_{VH} to I_{VV}; for scatterers in an orientationally isotropic environment and in the single scattering limit, the polarized scattered intensity is given by[23]

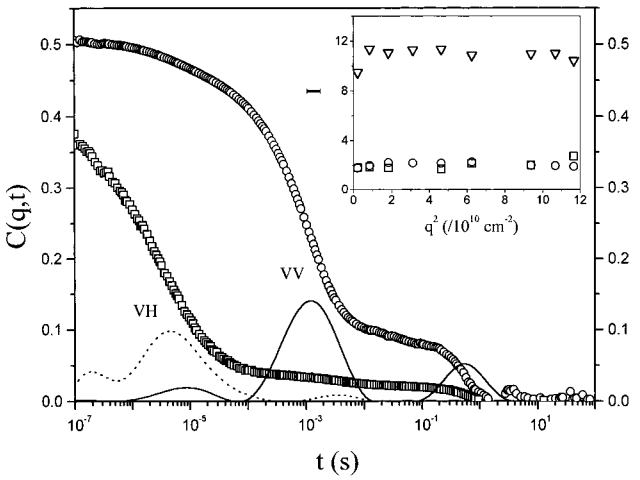

Figure 7. (a) Net normalized polarized (VV) (○) and depolarized (VH) (□) field correlation functions for a PPP-5 solution in toluene (36.9 mg/cm^3), along with the corresponding distributions of relaxation times, indicated by the solid and dotted lines, respectively. Inset: The comparison between the light-scattering intensities, I_f for the fast (○) and I_s for the slow (▽) VV process, as well as $^4/_3 I_{VH}$ for the depolarized slow process (□), at different q's.

$$I_{VV}(q) = I_{iso}(q) + {}^4/_3 I_{VH}(q) \tag{12}$$

The corresponding VH correlation function is also depicted in Figure 7, along with the distributions of relaxation times, as well as the intensities of the two VV modes and the $4/3I_{VH}$ contribution (inset of Figure 7). From the same intensity and dynamics, it is evident that the fast mode detected in toluene solutions in the VV correlation function originates from the orientational fluctuations of the system (see also inset of Figure 3). This information, which is necessary for avoiding misinterpretation, could be obtained only through the ability to measure VH dynamics and the combination of VV and VH measurements.

It is noted that the VH dynamics were detected only in toluene solutions and at $c > 25$ mg/cm^3, since at lower concentrations the molecular orientation time appeared to be faster than 10^{-7} *s*. However, at higher concentrations, it is possible to measure the dynamics of orientation fluctuations. A typical example is shown in Figure 8a (PPP-5, $c/c^* = 70$).

The VH correlation function appears to be much broader ($\beta_{KWW} \approx 0.4$) than the VV one. The large polydispersity of the samples can explain a much broader distribution of the orientation relaxation spectrum compared to the isotropic one, due to the corresponding stronger L dependence. An ILT analysis (eq 8) reveals two relaxation modes (inset of Figure 8a). The q dependence of the fast process cannot be truly assessed, since its dynamics fall into the short time edge of the correlator's window and its amplitude is too low; given this uncertainty, the fast process appears to be q-independent. The main mode becomes slower with increasing q (Figure 8b), as is also evident from the correlation functions of Figure 8a, which at larger q's relax within the time range of PCS. This unusual behavior has neither been predicted theoretically nor unambiguously observed experimentally; a seemingly similar observation has been briefly reported for PBLG solutions.[3] It is not trivial to rationalize physically a speed up of rotational diffusion at large length scales. The actual decrease of the slow reorientational rate with

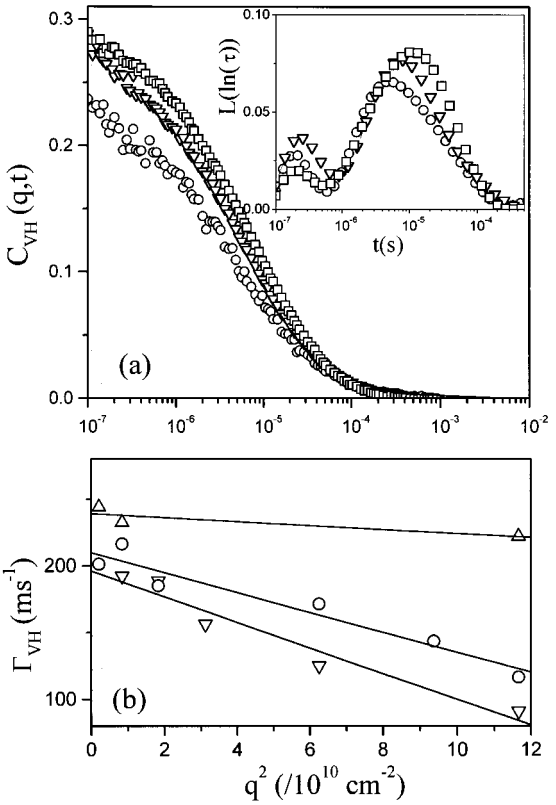

Figure 8. (a) Orientational time correlation functions for a semidilute solution of PPP-5 in toluene ($c/c^* = 70$), for different scattering angles [$\theta = 30°$ (○); $\theta = 90°$ (▽); $\theta = 150°$: (□)]. Inset: Corresponding distribution time relaxation function. (b) Variation of the rotational relaxation rate, Γ_{VH}, with q, at different concentrations of PPP-5 in toluene [$c/c^* = 29$ (△), 46 (○), 70 (▽)]. Solid lines represent linear fits.

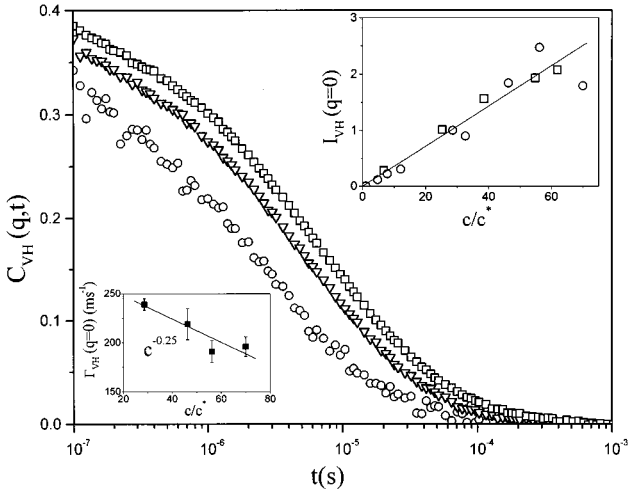

Figure 9. Orientational time correlation functions for PPP-5 solutions in toluene and different concentrations [$c/c^* = 26$ (○), 46 (▽), 56 (□)], at $q = 0.033$ nm^{-1}. Upper inset: Concentration dependence of the total VH intensity for solutions of PPP-5 in toluene (○) and chloroform (□). The solid line denotes the linear fit. Lower inset: Concentration dependence of the rotational relaxation rate, Γ_{VH}, at $q \rightarrow 0$, for PPP-5 solutions in toluene (■). The solid line represents the linear fit with slope −0.25.

q is depicted in Figure 8b, at different concentrations in the semidilute regime. The larger the concentration, the more pronounced this slowing down of the dynamics at large q's is, while the total I_{VH} is virtually q-independent for all examined concentrations. However, the VH intensity associated with the slow mode, exhibits a weak increase with q at the highest c; extending the measurements with these PPPs to even higher c's was precluded due to limited solubility.[20,54] This decrease of Γ_{VH} with q, along with the corresponding weak increase of I_{VH}, might imply orientational correlation in space due to some ordering of parts of these semistiff polymers, which can slow the orientational dynamics. A peak of the VH intensity at finite q was found to relate with orientationally correlated disclination lines in nematic liquid crystalline polymers.[55,56]

Figure 9 depicts the c dependence of the orientational correlation functions for the PPP-5 toluene solutions at $\theta = 150°$ ($qL \approx 2.5$). The total I_{VH} of PPP-5 in the thermodynamic limit ($q = 0$) in both solvents is shown as a function of c/c^* in the upper inset of Figure 9, whereas the lower inset depicts the decrease of Γ_{VH} with $c(q \rightarrow 0)$. The intensity increases linearly with c, assuming the same values. This finding suggests negligible pair orientation correlations, as the depolarized intensity is proportional to the number density and the intrinsic molecular anisotropy, excluding the possibility of excess VH scattering from cluster anisotropy; in the latter case, I_{VH} should be different in the two solvents. Further, the ratio of the translational diffusion (which is identified with the self-diffusion of the clusters) and slow rotational diffusion, D_s/D_r, decreases with concentration as can be seen from Figures 6 and 9 (their concentration, dependences are clearly different), suggesting that in toluene we do not observe the translation (VV) and the rotation (VH) of the same scatterer. In such a case, this ratio would either stay constant and approximately equal to the square of the hydrodynamic radius of the cluster, R_H^2, if for instance the diffusion constants of a sphere are used, or increase if equations such as (4) and (5) are used to describe the diffusion constants of the cluster. Thus, although the slow mode in VV originates from the translational diffusion of the small aggregates, which relaxes the composition fluctuations, the reorientational dynamics are controlled both inside and outside of the aggregates by the reorientation of the polymer molecules, which is constrained by their neighboring chains.

The significantly different orientational dynamics of PPPs in the two solvents over the examined c range needs justification. In the toluene solutions, scattering from regions with some orientational local ordering of the polymer chains dominates, leading to a slowing down of the rotational dynamics, with the peculiar q dependence of the slow decay rate discussed above. In this picture, the fast VH mode can be attributed to the average reorientation of the polymer chains that are not included in the clusters with locally increased orientational order; these chains reorient as they would in a semidilute isotropic solution of semistiff chains with no aggregates present. In chloroform solutions, we mainly see this kind of rotational relaxation, since the number of clusters or the areas with local orientation are not sufficient to affect the VH dynamics, up to $c/c^* \simeq 70$.

The rotational diffusion, as deduced from the slow VH mode in toluene solutions at $q = 0$, decreases as $c^{-0.25}$ over the rather narrow concentration range of our measurements (lower inset of Figure 9). Since the reorientational dynamics that we observe are probably seriously affected by nonmolecular factors, such as association or local ordering, it would not be reasonable to compare them with the predictions for the c dependence of rodlike particles. We should only mention that

even for such systems the rate is not expected to follow the c^{-2} behavior of the Doi−Edwards model in the whole semidilute and concentrated regime, but rather a weaker c dependence (c^{-1}) at low concentrations, and only for highly entangled solutions is the DE behavior reached.[14,18,22]

V. Concluding Remarks

The dynamics of concentration and orientation fluctuations of model hairy-rod poly(*p*-phenylenes) was probed with photon correlation spectroscopy, both in the polarized (VV) and depolarized (VH) geometries, in the semidilute regime. In VV, in addition to the cooperative diffusion, we detected the self-diffusion of small stable aggregates ($D_{slow} \sim c^{-1}$), as confirmed by independent pulse field gradient-NMR measurements. Thus, the Doi−Shimada−Okano description of the relaxation of concentration fluctuations was not confirmed. The dynamics helped significantly in obtaining the correct static information by isolating individual contributions to relaxation of concentration fluctuations. Up to $c/c^* \simeq 70$, which was the highest concentration reached before dissolution took place, the cooperative diffusion depended on $c^{0.9}$, a behavior intermediate to the flexible and rodlike predictions. Similarily, the osmotic modulus revealed a $c^{1.2}$ increase in the semidilure region, which is closer to the flexible chain behavior. The molecular self-diffusion coefficient scaled with $c^{-0.5}$, in qualitative agreement with the perturbation approaches in the early semidilute regime. Reorientational (VH) correlation functions were obtained at high concentrations in toluene and were dominated by a broad process exhibiting a slowing down at high q's and concentrations ($c^{-0.25}$). It was assigned to the molecular reorientation in the presence of some orientational correlations in space, due to local order of parts of the chains. These results provide important hints for the formulation of theories on the dynamics of such anisotropic systems and reveal the need for more depolarized measurements in a wider concentration range.

Acknowledgment. We are grateful to Professor M. Ballauff (University of Karlsruhe) for providing the polymers used in this work. We would also like to acknowledge the financial support of the EC (BRITE/EURAM program, contract CT91-0505) and the Greek General Secretariat for Research and Technology (Basic Research program, contract PENED-40).

References and Notes

(1) Doi, M.; Edwards, S. F. *The Theory of Polymer Dynamics*; Oxford University Press: New York, 1986.
(2) Tracy, M. A.; Pecora, R. *Annu. Rev. Phys. Chem.* **1992**, *43*, 525.
(3) Russo, P. S. In *Dynamic Light Scattering, The Method and some Applications*; Brown, B., Ed.; Clarendon Press: Oxford, U.K., 1993.
(4) Sato, T.; Teramoto, A. *Adv. Polym. Sci.* **1996**, *126*, 85.
(5) Seils, J.; Pecora, R. *Macromolecules* **1995**, *28*, 661.
(6) Buithenius, J.; Dhont, J. K. G.; Lekkekerker, H. N. W. *Macromolecules* **1994**, *27*, 7267.
(7) Drogemeier, J.; Hinsen, H.; Eimer, W. *Macromolecules* **1994**, *27*, 87. Drogemeier, J.; Eimer, W. *Macromolecules* **1994**, *27*, 96.
(8) Tinland, B.; Maret, G.; Rinaudo, M. *Macromolecules* **1990**, *23*, 596.
(9) Wang, L.; Garner, M. M.; Yu, H.; *Macromolecules* **1991**, *24*, 2368.
(10) Bu, Z.; Russo, P. S.; Tipton, D. L.; Negulescu, I. I. *Macromolecules* **1994**, *27*, 6871.
(11) Zero, K.; Pecora, R. *Macromolecules* **1982**, *15*, 87.
(12) DeLong, L. M.; Russo, P. S. *Macromolecules* **1991,** *24*, 6139.
(13) Maguire, J. F.; McTague, M. C.; Rondelez, F. *Phys. Rev. Lett.* **1981**, *47*, 148.
(14) Mori, Y.; Ookubo, N.; Hayakawa, R.; Wada, Y. *J. Polym. Sci., Polym. Phys. Ed.* **1982**, *20*, 2111.
(15) Keep, G. T.; Pecora, R. *Macromolecules* **1985**, *18*, 1167; **1988**, *21*, 817.
(16) McCarthy, T. F.; Witteler, H.; Pacula, T.; Wegner, G. *Macromolecules* **1985**, *54*, 337. Galda, P.; Rehahn, M. *Synthesis* **1996**, 614.
(17) Rehahn, M.; Schluter, A. D.; Wegner, G. *Macromol. Chem.* **1990**, *191*, 1991. Kallitsis, J. K.; Rehahn, M.; Wegner, G. *Macromol. Chem.* **1992**, *193*, 1021.
(18) Petekidis, G.; Fytas, G.; Witteler, H. *Colloid Polym. Sci.* **1994**, *272*, 1457.
(19) Petekidis, G.; Vlassopoulos, D.; Galda, P.; Rehahn, M.; Ballauff, M. *Macromolecules* **1996**, *29*, 8948. Tiesler, U.; Rehahn, M.; Ballauff, M.; Petekidis, G.; Vlassopoulos, D.; Maret, G.; Kramer, H. *Macromolecule* **1996**, *29*, 6832.
(20) Petekidis, G.; Vlassopoulos, D.; Fytas, G.; Kountourakis, N.; Kumar, S. *Macromolecules* **1997**, *30*, 919.
(21) Fixman, M. *Phys. Rev. Lett.* **1985**, *54*, 337; **1985**, *55*, 2429.
(22) Bitsanis, I.; Davis, H. T.; Tirrell, M. *Macromolecules* **1988**, *21*, 2824; **1990**, *23*, 1157.
(23) Berne, J. B.; Pecora, R. *Dynamic Light Scattering*; Wiley-Intersience Publications: New York, 1976.
(24) Broesma, S. *J. Chem. Phys.* **1960**, *32*, 1626; **1981**, *74*, 6989.
(25) Yamakawa, H.; Fujii, M. *Macromolecules* **1973,** *6*, 407. Hagerman, P. J.; Zimm, B. H. *Biopolymers* **1981**, *20*, 1481.
(26) Onsager, L. *Ann. N. Y. Acad. Sci.* **1949,** *51*, 627.
(27) Semenov, A. N.; Khokhlov, A. R. *Sov. Phys. Usp.* **1988**, *31*, 988.
(28) Yamakawa, H. *Moderm Theory of Polymer Solutions*; Harper and Row: New York, 1971.
(29) Coviello, T.; Burchard, W.; Dentini, M.; Crescenzi, V. *Macromolecules* **1987**, *20*, 1102.
(30) Bu, Z.; Russo, P. S. *Macromolecules* **1994**, *27*, 1187.
(31) Edwards, S. F.; Evans, K. E. *Trans. Faraday Soc.* **1982**, *78*, 113.
(32) Teraoka, I.; Hayakawa, R. J. *J. Chem. Phys.* **1988,** *89*, 1988.
(33) Sato, T.; Teramoto, A. *Macromolecules* **1991**, *24*, 193.
(34) Sato, T.; Takada, Y.; Teramoto, A. *Macromolecules* **1991**, *24*, 6262.
(35) Odijk, T. *Macromolecules* **1983**, *16*, 1340; **1984**, *17*, 502.
(36) Doi, M. *J. Polym. Sci., Polym. Symp.* **1985**, *73*, 93.
(37) Semenov, A. N. *J. Chem. Soc., Faraday Trans. 2* **1986**, *82*, 317.
(38) Shimada, T.; Doi, M.; Okano, K. *J. Chem. Phys.* **1988**, *88*, 2815. Doi, M.; Shimada, T.; Okano, K. *J. Chem. Phys.* **1988,** *88*, 4070. Shimada, T.; Doi, M.; Okano, K. *J. Chem. Phys.* **1988,** *88*, 7181.
(39) Maeda, T. *Macromolecules* **1989**, *22*, 1881. Maeda, T. *Macromolecules* **1990**, *23*, 1464.
(40) Provencher, S. W. *Macromol. Chem.* **1979**, *180*, 201.
(41) Callaghan, P. T. *Principles of Nuclear Magnetic Resonance Microscopy*; Clarendon Press: Oxford, U.K., 1992.
(42) De Gennes, P. G. *Scaling Concepts in Polymer Physics*; Cornell University Press: Ithaca, NY, 1979.
(43) Jinbo, Y.; Sato, T.; Teramoto, A. *Macromolecules* **1994**, *27*, 6080.
(44) Seghrouchni, R.; Petekidis, G.; Vlassopoulos, D.; Fytas, G.; Semenov, A. N.; Roovers, J.; Fleisher, G. Submitted for publication to *Europhys. Lett.*
(45) Merkle, G.; Burchard, W.; Lutz, P.; Freed, K. F.; Gao, J.; *Macromolecules* **1993**, *26*, 2736.
(46) Ishihara, A.; Hayashida, T. *J. Polym. Sci., Part C* **1951,** *6*, 40.
(47) Richtering, W.; Gleim, W.; Burchard, W. *Macromolecules* **1992**, *25*, 3795.
(48) Fujime, S.; Takasaki-Ohsita, M.; Maeda, T. *Macromolecules* **1987**, *17*, 1157.
(49) Goinga, H. Tj.; Pecora, R. *Macromolecules* **1991,** *24*, 6128.
(50) Pusey, P. N.; Tough, R. J. A. In *Dynamic Light Scattering, Applications of Photon Correlation Spectroscopy*; Pecora, R., Ed.; Plenum Press: New York, 1985.

(51) Jian, T.; Anastasiadis, S. H.; Semenov, A. N.; Fytas, G.; Fleisher, G.; Vilesov, A. D. *Macromolecules* **1995**, *28*, 2439.
(52) Chu, B. *Laser Light Scattering*; Academic Press: London, 1974.
(53) Benmuna, M.; Duval, M.; Benoit, H.; Akcasu, Z. *Macromolecules* **1987**, *20*, 1107. Zhou, P.; Brown, W. *Macromolecules* **1990**, *23*, 1131. Jian, T.; Anastasiadis, S. H.; Rizos, A. K.; Fytas, G.; Akcasu, Z. *J. Chem. Phys.* **1994,** *101*, 3222.
(54) Petekidis, G.; Vlassopoulos, D.; Fytas, G.; Rulkens, R.; Wegner, G.; Fleisher, G. Manuscript in preparation.
(55) Hashimoto, T.; Nakai, A.; Shiwaku, T.; Hasegawa, H.; Rojsaczer, S.; Stein, R. S. *Macromolecules* **1989**, *22*, 422.
(56) Greco, F. *Macromolecules* **1989**, *22*, 4622.

MA9711295